

Resonant Raman scattering in the $\text{Pb}_2\text{Sr}_2(\text{Y,Ca})\text{Cu}_3\text{O}_{8+\delta}$ superconductor

E. T. Heyen, R. Liu, M. Garriga, B. Gegenheimer, C. Thomsen, and M. Cardona

Max-Planck-Institut für Festkörperforschung, Heisenbergstrasse 1, D-7000 Stuttgart 80, Federal Republic of Germany

(Received 26 June 1989)

We have measured resonant phonon Raman profiles of a superconducting $\text{Pb}_2\text{Sr}_2\text{Y}_{0.75}\text{Ca}_{0.25}\text{Cu}_3\text{O}_{8+\delta}$ crystal for laser energies from 1.65 to 2.7 eV. The resonances at 1.75 and 2.55 eV and the rise towards the uv, also seen in ellipsometry, are assigned to transitions involving the $\text{Cu}(2)$ $d_{x^2-y^2}-\text{O}(3)$ $p_{x,y}$, and $\text{Pb}-\text{O}(1)$ complexes. There exists a relationship between the phonon-induced atomic motions and the location in the unit cell of the electronic transition. We also assign additional peaks that appear under resonant conditions.

In the past, resonant Raman scattering has been used as a tool to investigate electronic band structures as well as vibrational properties, mainly in semiconductors.¹ Resonant Raman measurements for high- T_c materials are important since their band structures are little known. There do exist one-electron calculations,² but there is still uncertainty in the assignment of observed electronic transitions.³ Here we report resonant Raman and ellipsometric data for Pb-based superconductors and related insulators⁴ which yield information about the electronic structure.

Using rotating-analyzer ellipsometry, we obtained the dielectric functions to lead-based ceramics. Figure 1, displaying a $\text{Pb}_2\text{Sr}_2\text{SmCu}_3\text{O}_8$ spectrum, exhibits peaks at 1.75, 2.6 (also seen in $\text{YBa}_2\text{Cu}_3\text{O}_{6+\delta}$), 3.4, and 3.9 eV. ϵ_2 increases strongly between 2.5 and 4 eV.

Neutron powder diffraction and electron microscopy⁵ show that the orthorhombic distortion of $\text{Pb}_2\text{Sr}_2\text{YCu}_3\text{O}_8$ originates from the displacement of the oxygen atoms in the PbO planes. This leads to a non- c -centered, orthorhombic, primitive cell with twice the size of the original pseudotetragonal cell (shown in Fig. 2). If the crystal were c centered without O displacements, D_{2h} -point-group factor-group analysis would yield $6A_g + B_{1g} + 7B_{2g} + 7B_{3g}$ Raman-active, $7B_{1u} + 8B_{2u} + 8B_{3u}$ infrared-active, one silent A_u , and three acoustic vibrational modes.⁶ The $6A_g + B_{1g}$ modes have previously been assigned,⁷ while, as in all other high- T_c superconductors, the B_{2g} and

B_{3g} modes seem to be too weak to be clearly detected. Since the non- c -centered character shows up predominantly in the PbO planes, the distortions should only create additional vibrational modes involving those planes. If we assume a non- c -centered displacement of the oxygen atoms along the b axis, group-theoretical analysis for a pair of Pb_2O_2 planes with C_{2v} symmetry shows that each c -centered B_{2u} mode, involving Pb or O vibrations along the a direction, becomes Raman active at the (orthorhombic) zone center and at the [010] zone edge as well as at the [010] zone edge of the corresponding acoustic branch in such a way that its Raman tensor is the same as for D_{2h} -symmetry B_{1g} mode. Likewise, the B_{3u} modes become Raman active at these points, but show A_g -type Raman tensors. Therefore, for each $B_{2u}-B_{3u}$ pair of infrared-active modes, we might expect $(3B_{1g} + 3A_g)$ -type Raman-active modes. Similarly, the zone-boundary modes corresponding to each A_g mode involving motion of the $\text{Pb}-\text{O}(2)$ plane become Raman active too. These

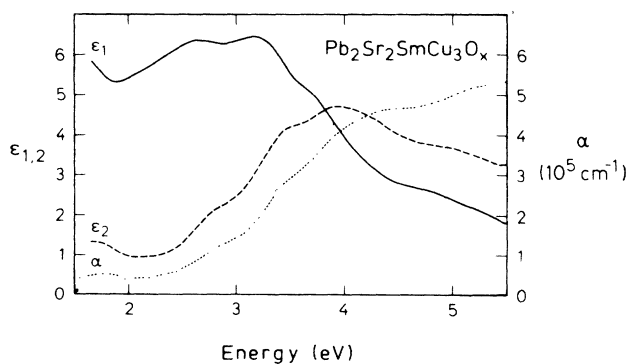


FIG. 1. Dielectric function of $\text{Pb}_2\text{Sr}_2\text{SmCu}_3\text{O}_8$ (ϵ_1 , solid line; ϵ_2 , dashed line; absorption coefficient α , dotted line).

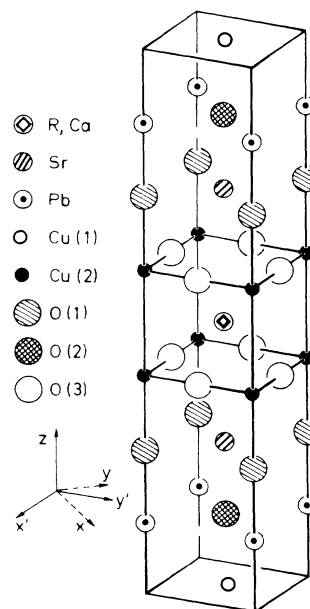


FIG. 2. Pseudotetragonal unit cell with the $\text{O}(2)$ atoms at the ideal rocksalt position.

modes may be observed, especially in the case of resonance.

A further source of symmetry reduction (i.e., more Raman-active phonons) is the uncertainty about the site of the oxygen atoms in excess of O_8 , always present in the material. It was argued⁴ that excess oxygen is located in the otherwise empty Cu(1) plane. If this oxygen is not deposited in an ordered fashion, there should exist more detectable Raman-active Cu(1)- O_{excess} and Pb- O_{excess} vibrations, probably with a poorly defined polarization.

We were able to grow rather large ($2.5 \times 2.5 \times 0.5 \text{ mm}^3$) and extremely pure orthorhombic, partially twinned crystals from a PbO-CuO flux.⁴ The crystal used had $T_c \approx 20 \text{ K}$ and $a = 5.371(6) \text{ \AA}$, $b = 5.457(6) \text{ \AA}$, and $c = 15.708(2) \text{ \AA}$.

Their Raman spectra for several polarization geometries have been measured for 14 wavelengths from 4579 to 7525 \AA (Ar^+ and Kr^+ lasers) at temperatures ranging from 10 to 295 K. Figure 3 shows the spectra taken at 10 K for different laser wavelengths in $z(x'x')\bar{z}$ polarization, where x', y' denote the pseudotetragonal axes and x, y the actual orthorhombic axes. Absolute as well as relative peak intensities vary drastically when changing the excitation frequency. The spectrum taken at $\lambda_L = 5145 \text{ \AA}$ where, as we will see later, resonance effects are small, shows the $6A_g$ modes at 80, 150, 250, 435, 484, and 570 cm^{-1} , the B_{1g} mode at 325 cm^{-1} , and an additional doublet peak at 180 and 190 cm^{-1} . In a previous paper,⁷ we assigned the $6A_{1g} + B_{1g}$ peaks to vibrations of the Pb, Cu(2)-Sr in- and out-of-phase, O(3) in-phase, O(2), O(1), and O(3) out-of-phase, respectively. The origin of the 180 and 190- cm^{-1} peak, only observed at low T , remained unclear.

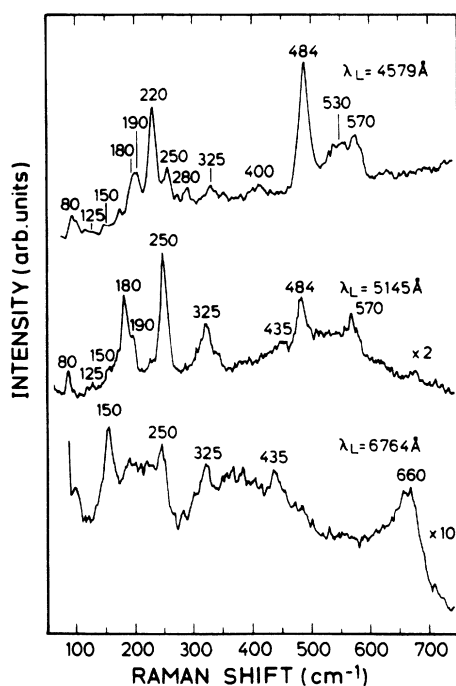


FIG. 3. Raman spectra for laser wavelengths of 4579, 5145, and 6764 \AA taken at 10 K in $z(x'x')\bar{z}$ geometry.

For $\lambda_L = 4579 \text{ \AA}$, five additional peaks at 125, 220, 280, 400, and 530 cm^{-1} are seen. The peaks at 125, 400, and 530 cm^{-1} are observed only in $z(x'x')\bar{z}$ and $z(xx)\bar{z}$ geometries. Their Raman tensor is therefore that of D_{2h} -symmetry A_g mode. In contrast, the peaks at 220 and 280 cm^{-1} , detectable only in $z(x'x')\bar{z}$ and $z(xy)\bar{z}$ geometries, are of B_{1g} type. For $\lambda_L = 6764 \text{ \AA}$, an additional broad A_g -type peak is observed at 660 cm^{-1} . A similar structure is also seen in $\text{YBa}_2\text{Cu}_3\text{O}_6$.⁸

For all laser wavelengths, the $x'(zz)\bar{x}'$ spectra just show the very strong 570- cm^{-1} peak and the much weaker ones at 484, 150, and 80 cm^{-1} , while the $x(zy)\bar{x}$ spectrum has no clearly identifiable structures. Therefore, even under resonant conditions, the B_{2g} and B_{3g} modes are too weak to be observed. Only the Raman tensor of the 570- cm^{-1} mode has a clearly dominating zz component while the 480- cm^{-1} peak does not, thus indicating that the motion of O(1) (480 cm^{-1}) and the O(2) (570 cm^{-1}) atoms cannot couple to the same electronic bands. Usually, only the Cu-O stretch in the z direction generates Raman tensors with strong zz components. We have found that other Pb-based ceramic samples, with different rare earths and varying oxygen contents, prepared by different groups, all show similar peaks.

We obtained resonance spectra for all observed peaks by taking the peak heights measured in the $z(x'x')\bar{z}$ configuration at 10 K and normalizing them against the known BaF_2 Raman phonon profile.⁹ The resonance profiles were not corrected for changes in absorption and reflectivity since ellipsometry data (Fig. 1) showed that the small bumps in the nearly flat spectra of their coefficients around 1.75 and 2.6 eV would even enhance the features obtained without correction. Figure 4(a) shows the resonance profiles for what we believe to be the $6A_g + B_{1g}$ modes of the nondistorted orthorhombic cell. It can be seen that the peaks at 150 and 250 cm^{-1} resonate at 1.75 and 2.55 eV, the 325- cm^{-1} mode at 1.75 and 2.5 eV, and the 435- cm^{-1} line at 1.75 and 2.4 eV, while the 80- cm^{-1} structure and the two high-frequency modes resonate only weakly at 1.75 eV but exhibit a steep rise towards the uv. Preliminary measurements of the $x'(zz)\bar{x}'$ resonance profiles indicate that strong resonances do not exist in this geometry.

Recently, Kress *et al.* have performed lattice-dynamical calculations for $\text{Pb}_2\text{Sr}_2\text{YCu}_3\text{O}_8$,¹⁰ showing excellent agreement with the $6A_g + B_{1g}$ Raman modes. We will now use the phonon eigenvectors calculated there to analyze the resonance behavior of the phonons.

We note that all modes that involve, according to Ref. 10, a strong vertical motion in the Cu(2)-O(3) plane, e.g., the 150-, 250-, 325-, and 435- cm^{-1} lines, show resonances near 1.75 and 2.55 eV. The 80- and 484- cm^{-1} modes that involve small CuO_2 plane atom displacements, resonate weakly. Similarly, we observe that the 484- cm^{-1} peak, mainly a stretching of the Pb-O(1) bond, resonates very strongly towards the uv. The $x'x'$ component of the 570- cm^{-1} -mode Raman tensor and the 80- and 150- cm^{-1} lines, involving a smaller stretching of this bond, resonate more weakly in the uv. This resonance that should also exist in the 250- cm^{-1} -mode profile seems to be masked by the very strong 2.55-eV resonance.

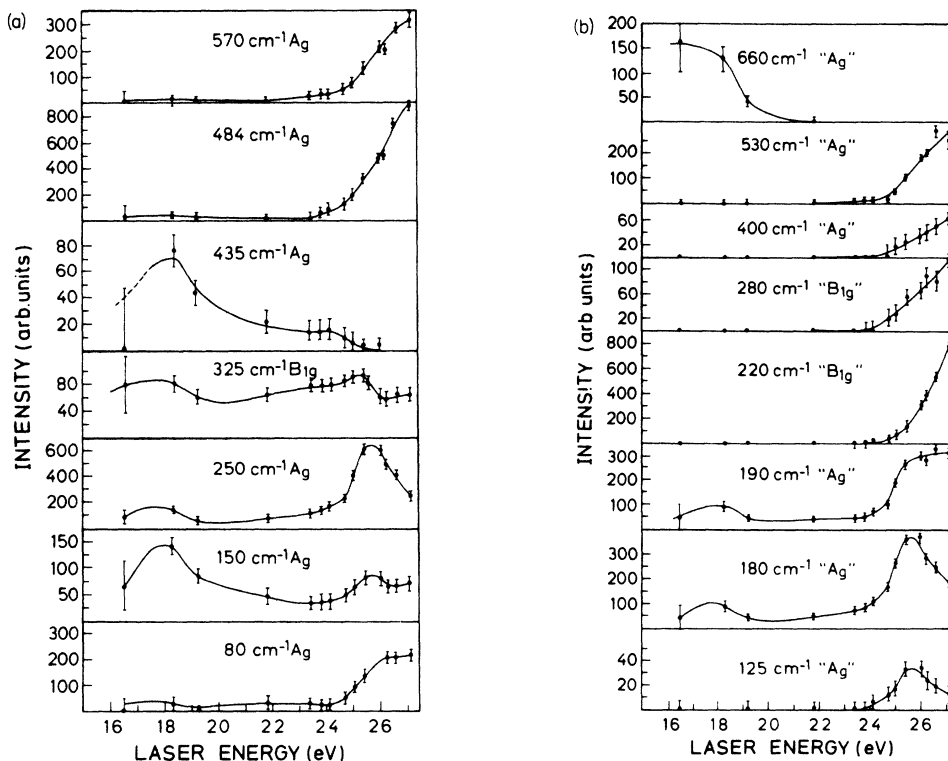


FIG. 4. Resonant Raman profiles for (a) the $6A_g + B_{1g}$ modes and (b) additional modes, all taken at 10 K in $z(x'x')\bar{z}$ geometry. Polarization selection rules are indicated as A_g or B_{1g} type. The y -axis calibration is the same for all profiles.

We note that the resonance energies are close to those of critical points seen in ellipsometry (Fig. 1). In addition, we conclude that there is a close relationship between the sites of the atoms which move the most for a given phonon and the predominant location in real space of resonant electronic transitions. This effect becomes possible because the unit cell is so large that the coupling between far away regions is weak. We can therefore assign the 1.75- and 2.55-eV transitions to happen within the Cu(2) $d_{x^2-y^2}$ -O(3) $p_{x,y}$ complex. These Cu d -O p bands cannot produce the $z(xx)\bar{z}$ Raman activity, involving vertical motion of the Cu-O plane, since there is no change of the sum of the polarizabilities of these bonds linear in atomic displacements. The Raman activity involving O(2)-O(3) motion is most likely induced by the asymmetric crystal field generated by the Y^{3+} and Sr^{2+} ions. The weak resonance near 2.5 eV of the 325- and 435- cm^{-1} lines, involving primarily O(3) displacements, is red shifted by 50 and 150 meV, respectively, with respect to the strong resonance of the 150- and 250- cm^{-1} modes. A similar behavior was previously observed in semiconductors,¹¹ and can be explained by the interference of the resonant Raman polarizability with a nonresonant background: The position of the resonance maximum can shift by as much as a linewidth.

The uv resonance can be assigned to a transition from the O(1) $2p$ to the Pb $6p$ level. Since p_x - p_x , p_y - p_x , and p_z - p_z transitions are symmetry forbidden for light propagating along the z axis [because of the mirror planes along the O(1)-P bonds], the resonant transitions must be $p_{x,y}$

to p_z , or p_z to $p_{x,y}$.

These conclusions are supported by the recent linear-augmented-plane wave band-structure calculations of Mattheiss and Hamann,² which show a peak in the Pb $6p_z$ -O(1) partial density of states at the X - M - Γ - Z line between 1.3 and 1.7 eV above the Fermi energy and for O(1) $2p$ between 1.6 and 2.1 eV below E_F resulting in transition energies between 2.9 and 3.8 eV, compatible with the steep rise towards the uv we observe. Similarly the calculations show that transitions lower than 2.6 eV are only possible within the Cu(2) $d_{x^2-y^2}$ -O(2) $p_{x,y}$ complex. Unfortunately, it does not seem possible to extract more detailed information from this local-density-approximation-type calculation which is afflicted by "gap problems"¹² and does not include the strong correlation of the Cu d electrons.

Finally, we attempt an assignment of the additional peaks observed under resonant conditions. Their resonance behavior, shown in Fig. 4(b), is similar to that of the phonons from the c -centered unit cell [Fig. 4(a)]. In addition, all modes have a definite A_g - or B_{1g} -type symmetry. It is therefore very unlikely that they are caused by impurities or other phases. The modes observed at 220, 280, 400, and 530 cm^{-1} , showing a uv resonance, must involve a motion of the Pb-O(2) plane. The lattice-dynamical calculation¹⁰ states the existence of Pb-O(2) B_{2u} - B_{3u} modes at 366 and 485 cm^{-1} . Using group theory as described above, we can therefore tentatively assign the A_g -type peaks at 400 and 530 cm^{-1} and those of B_{1g} type at 280 and 220 cm^{-1} as the tetragonal zone center and

zone boundary B_{2u} - B_{3u} modes, respectively, that become Raman active due to the non- c -centered distortion, strongly enhanced by resonance.

The 180- and 190- cm^{-1} lines exhibit the same resonance behavior, symmetry, and energy range as the very strong 250- cm^{-1} mode. Since the latter also involves O(2) motion, it "feels" the non- c -centered distortion. We therefore conjecture that the 180- and 190- cm^{-1} peaks are the zone-boundary modes corresponding to the 250- cm^{-1} peak. A problem with this assignment comes from the fact that the 180- and 190- cm^{-1} peaks are rather strong (half of the 250- cm^{-1} intensity) and are also observed away from resonance. The origin of the 125- cm^{-1} peak, showing exclusively the 2.55-eV resonance remains unclear, but it might be a resonance-induced infrared-active mode (Ref. 10 calculated 121 cm^{-1}) involving a motion of the Cu(2)-O(3) plane as well as of the displaced O(2) atom. The A_g -type 660- cm^{-1} mode resonant at 1.75 eV is especially interesting since a mode at a similar frequency appears also in $\text{YBa}_2\text{Cu}_3\text{O}_6$.⁸ The fact that this peak is rather broad ($\approx 50 \text{ cm}^{-1}$) indicates that it may be a two-phonon process, perhaps the overtone of the 325- cm^{-1} B_{1g} mode which is also resonant at 1.75 eV.

Finally, we mention that the intensity of the peaks at

180, 190, 220, 280, 400, and 530 cm^{-1} , which are, according to our assignments, all induced by the non- c -centered displacement at the O(2) atoms, decreases with increasing temperature, suggesting that the distortion of the unit cell is a decreasing function of temperature.

In conclusion, after finding a close correlation between the site of resonating phonon-induced atomic motion and the site of the electronic transition, we have assigned the 1.75- and 2.55-eV transitions to occur within the Cu(2) $d_{x^2-y^2}$ -O(3) $p_{x,y}$ complex, while the uv transition involves the Pb $6p_z$ -O(1) complex. Finally, we have assigned additional Raman peaks detected under resonant conditions to be either due to the non- c -centered distortion of the PbO planes or to an overtone of the 325- cm^{-1} B_{1g} mode. In view of the poor knowledge of the electronic band structure, our interpretation is to be regarded as preliminary. Measurements with tunable lasers and further into the uv, in particular on simpler materials such as $\text{YBa}_2\text{Cu}_3\text{O}_{7-\delta}$, are on the way in order to clarify matters.

We are pleased to thank W. Kress and J. Kircher for valuable discussions and H. Hirt, M. Siemers, and P. Wurster for expert technical help.

¹See, for a review, *Light Scattering in Solids II*, edited by M. Cardona and G. Güntherodt (Springer-Verlag, Berlin, 1982).

²For $\text{Pb}_2\text{Sr}_2\text{YCu}_3\text{O}_8$, L. F. Mattheiss and D. R. Hamann, *Phys. Rev. B* **39**, 4780 (1989).

³For $\text{YBa}_2\text{Cu}_3\text{O}_{7-\delta}$, M. Garriga, J. Humlíček, J. Barth, R. L. Johnson, and M. Cardona, *J. Opt. Soc. Am.* **6**, 470 (1989); or J. Kircher, M. Alouani, M. Garriga, P. Murugaraj, J. Maier, C. Thomsen, M. Cardona, O. K. Andersen, and O. Jepsen, *Phys. Rev. B* **40**, 7368 (1989).

⁴R. J. Cava, B. Battlog, J. J. Krajewski, L. W. Rupp, L. F. Schneemeyer, T. Siegrist, R. B. van Dover, P. Marsh, W. F. Peck, Jr., P. K. Callagher, S. H. Gharenn, J. H. Marshall, R. C. Farrow, J. V. Waszcak, R. Hull, and P. Trevor, *Nature (London)* **336**, 211 (1988).

⁵R. J. Cava, M. Marezio, J. J. Krajewski, W. F. Peck, Jr., A. Santoro, and F. Beeck, *Physica C* **157**, 272 (1989); E. A. Hewat, J. J. Capponi, R. J. Cava, C. Chailout, M. Marezio, and

J. L. Tholence, *ibid.* **157**, 509 (1989).

⁶C. Thomsen, M. Cardona, R. Liu, Hj. Mattausch, W. König, F. Garcia-Alvaredo, B. Suarez, E. Moran, and M. Alario-Franco, *Solid State Commun.* **69**, 857 (1989).

⁷R. Liu, M. Cardona, B. Gegenheimer, E. T. Heyen, and C. Thomsen, *Phys. Rev. B* **40**, 2654 (1989).

⁸E. T. Heyen (unpublished).

⁹J. M. Calleja, H. Vogt, and M. Cardona, *Philos. Mag. A* **45**, 239 (1982).

¹⁰W. Kress, U. Schröder, J. Prade, A. D. Kulkarni, and F. W. de Wette, in *Proceedings of the Conference on High Temperature Superconductors, Stanford, 1989*, edited by W. A. Harrison, N. E. Philips, and R. N. Shelton [Physica C (to be published)].

¹¹W. Kauschke, N. Mestres, and M. Cardona, *Phys. Rev. B* **36**, 7469 (1987).

¹²L. J. Sham and M. Schluter, *Phys. Rev. Lett.* **51**, 1888 (1983).